

Numerical Modeling for Comparison of Emitter-Base Designs of InGaP/GaAs Heterojunction Bipolar Transistors

Juan M. López-González

Micro and Nano Technologies Group, Centre for Research in NanoEngineering,
 Universitat Politecnica de Catalunya, Campus Nord
 Calle Jordi Girona 1, 08034 Barcelona, Spain, jmlopezg@eel.upc.edu

ABSTRACT

In this paper, using physics based two-dimensional numerical simulator ATLAS, DC and AC performances of InGaP/GaAs heterojunction bipolar transistors, which have very similar cut-off frequency and maximum oscillation frequency, are evaluated. Numerical device modeling is used for comparison of emitter-base designs of InGaP/GaAs heterojunction bipolar transistors.

Keywords: InGaP/GaAs, heterojunction bipolar transistor, semiconductor device modeling, numerical modeling.

1 INTRODUCTION

Heterojunction bipolar transistors (HBTs) extend the advantages of silicon bipolar transistors to significantly higher frequencies. They are used in applications requiring high current capacities, high transconductance, high voltage handling capability, low noise and uniform threshold voltage [1]-[2]. The InGaP/GaAs HBT is an important investigation topic in power amplifiers [3]-[4], but the technology is also applicable to low noise amplifiers in the range of frequencies from 2 to 6 GHz. Reference [5] shows results of an LNA for WLAN applications at 5.3 GHz with 13 dB gain, noise figure of 2.1 dB and excellent linearity in terms of IIP3.

Numerical modeling of semiconductor devices allows to deep in the implications that the geometry and the characteristics of the materials have in the real operation of the device [6]-[7]. Several geometric implications of the InGaP/GaAs HBT design have been studied, theoretical and experimentally, in order to obtain better device performance [8]-[9]. In this work, the consequences of the design of the emitter pedestal in the electric DC and AC performance of InGaP/GaAs HBTs are studied using physics based two-dimensional numerical modeling TCAD tool, ATLAS [10].

2 DEVICES

Two heterojunction bipolar transistors are studied. Both devices are 1 emitter finger, two base contacts -1 μm length each one- and two collector contacts -4 μm length each one-, and they have the collector area of $18.6 \times 20 \mu\text{m}^2$ and

the base pedestal area of $6.6 \times 20 \mu\text{m}^2$. Other dimensions of the device DEV-A are: spacing between emitter mesa and base contact, L_{BE} , is 1.3 μm , emitter pedestal area, A_{PE} , is $2 \times 20 \mu\text{m}^2$ and emitter contact area, A_E , is $1 \times 20 \mu\text{m}^2$. The particular dimensions of the device DEV-B are: spacing between emitter mesa and base contact, L_{BE} , is 1 μm , emitter pedestal area, A_{PE} , is $2.6 \times 20 \mu\text{m}^2$ and emitter contact area, A_E , is $2 \times 20 \mu\text{m}^2$. Figure 1 shows geometry of the device DEV-A.

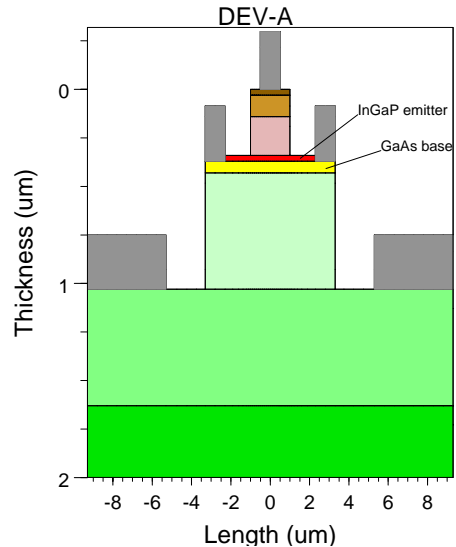


Figure 1: Geometry of the DEV-A, InGaP/GaAs HBT.

Doping profile of the InGaP/GaAs HBT transistors is in Table 1 and it is used for applications up to 10 GHz [11].

| MATERIAL | THICKNESS(Å) | DOPING (cm ⁻³) |
|---------------|--------------|----------------------------|
| n-InGaAs | 300 | 1e19 |
| n-GaAs | 1100 | 1e19 |
| n-GaAs | 2000 | 2e17 |
| n-InGaP | 300 | 4.5e17 |
| p-GaAs | 600 | 4e19 |
| n-GaAs | 6000 | 1.5e16 |
| n-GaAs | 6000 | 3e18 |
| Sust.-GaAs | - | - |

Table 1: Doping profile of NPN InGaP/GaAs HBTs.

| | GaAs | GaAs | InGaP | GaAs-p | GaAs | GaAs |
|---|------|------|-------|-----------|------|------|
| E_g (eV) | 1.42 | 1.42 | 1.84 | 1.42-0.07 | 1.42 | 1.42 |
| χ (eV) | 4.07 | 4.07 | 3.93 | 4.07 | 4.07 | 4.07 |
| ϵ_r | 13.2 | 13.2 | 12.5 | 13.2 | 13.2 | 13.2 |
| N_c (10^{17} cm^{-3}) | 4.5 | 4.5 | 8.4 | 4.5 | 4.5 | 4.5 |
| N_v (10^{19} cm^{-3}) | 1 | 1 | 1 | 1 | 1 | 1 |
| μ_n ($\text{cm}^2\text{V}^{-1}\text{s}^{-1}$) | 1600 | 3000 | 850 | 1200 | 4000 | 2000 |
| μ_p ($\text{cm}^2\text{V}^{-1}\text{s}^{-1}$) | 100 | 200 | 70 | 60 | 200 | 120 |
| τ (10^{-9} s) | 0.5 | 1 | 0.5 | 0.05 | 1 | 1 |

Table 2: Material parameters used in the simulation of the InGaP/GaAs HBTs.

In this study, it stays constant the total size of the device, the dimensions of the base mesa structure and the doping profile and it is only modified the layout of the emitter and base regions, see Fig. 2. The results show that it is possible keeping IC rules of design of the transistor layout and it does not changing the wafer area, optimize the heterojunction bipolar transistor design.

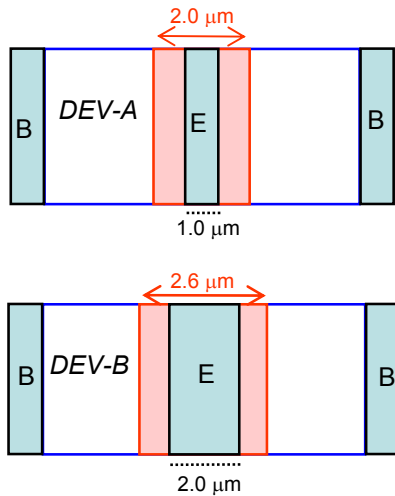


Figure 2: Emitter-base designs of the InGaP/GaAs HBTs.

3 MODELING

Numerical modeling of heterojunction bipolar transistors can help to understand the physical behavior of the device and optimize its design. In this work using physics based two-dimensional numerical modeling TCAD tool, ATLAS, emitter-base designs of InGaP/GaAs HBTs are studied. The model solves the Poisson and the electron and hole continuity equations assuming Anderson affinity-rule and band gap narrowing in the high doped base region

[6]. Material parameters of HBTs used in the simulation are in Table 2. They were extracted from [12]. Figure 3 shows equilibrium energy band diagram for the InGaP/GaAs HBTs.

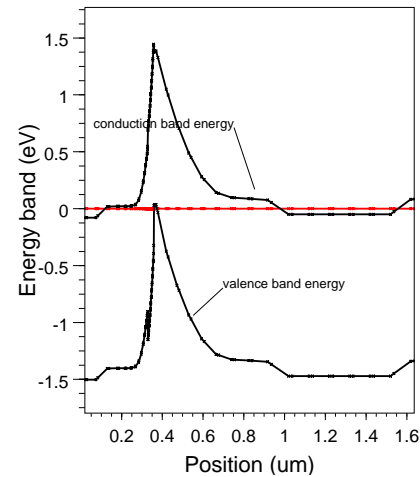


Figure 3: Equilibrium energy band of the InGaP/GaAs HBTs under the emitter contact.

4 DC AND AC RESULTS

Heterojunction bipolar transistors DC performance is illustrated by Figure 4 and Table 3. Forward gain current of the device DEV-A is higher than that of the device DEV-B. Values of $\beta_{F,max}$ of 160 and 100, respectively, are getting. Offset collector-emitter voltage, $V_{CE,off}$, of DEV-B is smaller than that of the device DEV-A due to the size difference among emitter area to collector area in the device DEV-B is smaller than that in the device DEV-A. Base-emitter on-voltages are also different, for example at the

collector current of 1 nA, these are 0.92 V for device DEV-A and 0.9 V for device DEV-B.

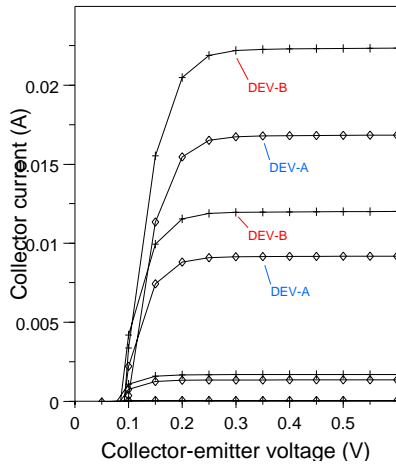


Figure 4: $I_c(V_{ce})$ plots for devices DEV-A (rhombus marks) and DEV-B (plus marks).

| | DEV-A | DEV-B | |
|-----------------|-------|-------|-----------|
| $\beta_{F,max}$ | 160 | 100 | |
| $V_{CE,offset}$ | 0.12 | 0.1 | $I_c@5mA$ |
| $V_{BE,on}$ | 0.92 | 0.9 | $I_c@1nA$ |

Table 3: DC performance of the InGaP/GaAs HBTs.

Table 4 and figures 5 and 6 present AC performance of the HBTs, being $I_C = 26$ mA and $V_{CE} = 2.5$ V. Both HBTs have approximately $f_T = 94$ GHz and $f_{max} = 84$ GHz, estimated at the frequency of 2.5 GHz. Above of approximately 10 GHz, HBTs are unconditionally stable. But different AC performance is observed, for example, in the maximum transducer gain and the maximum stable gain.

| 2.5 GHz | DEV-A | DEV-B |
|------------------------|-------|-------|
| K_{Stern} | 0.15 | 0.20 |
| h_{fe} (dB) | 37.4 | 37.8 |
| GU (dB) | 33.5 | 33.7 |
| G_{mT} (dB) | 36.2 | 34.3 |
| MSG (dB) | 25.3 | 27.2 |
| Input Loss (dB) | -1.34 | -2.50 |
| Output Loss (dB) | -1.28 | -2.26 |
| Forward Gain (dB) | 24.5 | 26.8 |
| Reverse Isolation (dB) | -26.2 | -27.5 |

Table 4: AC performance of InGaP/GaAs HBTs at 2.5 GHz.

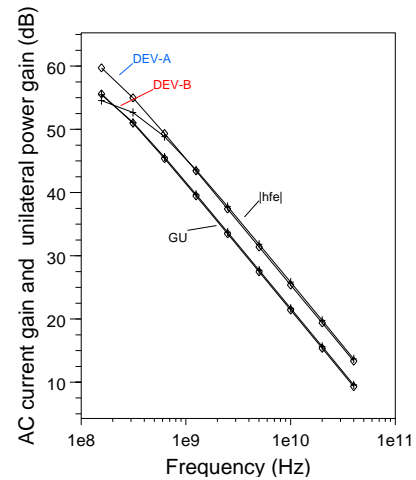


Figure 5: AC current gain, $|h_{fe}|$, and Unilateral Power Gain, GU, as a function of the frequency, for devices DEV-A (rhombus marks) and DEV-B (plus marks).

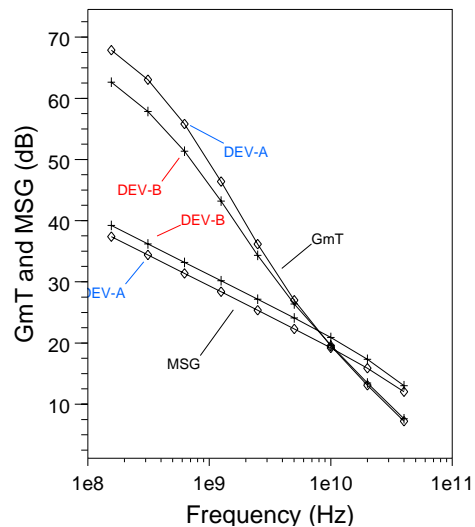


Figure 6: Maximum transducer power gain, G_{mT} , and maximum stable gain, MSG, as a function of the frequency for devices DEV-A (rhombus marks) and DEV-B (plus marks).

RF device performance at 2.5 GHz can be explained as follows. Susceptance of the device DEV-A is smaller than that in the device DEV-B since that DEV-A have emitter contact area smaller than device DEV-B, in consequence smaller capacity. Moreover, conductance of the DEV-A is also smaller than that in the device DEV-B because DEV-A has pedestal region area smaller and distance between electrodes larger than in the device DEV-B. Output admittance behavior is qualitatively similar that of the input admittance, although quantitatively less important due to the distance between the contacts of the collector and emitter.

In order to explain the RF gain versus the frequency performance of the HBTs observed in the figure 6, it is included the figure 7. This figure shows the forward gain, S_{21} , and the reverse isolation, S_{12} , as a function of the frequency. Note that below 4 or 5 GHz, the value of S_{21} of the device DEV-B is higher than that in the device DEV-A and that above those frequencies S_{12} –reverse gain- of the device DEV-B is smaller than in the device DEV-A. The combined effect of these two parameters reverts in the maximum stable gain imposing this advantage by DEV-B design in front of DEV-A design in the studied frequencies range.

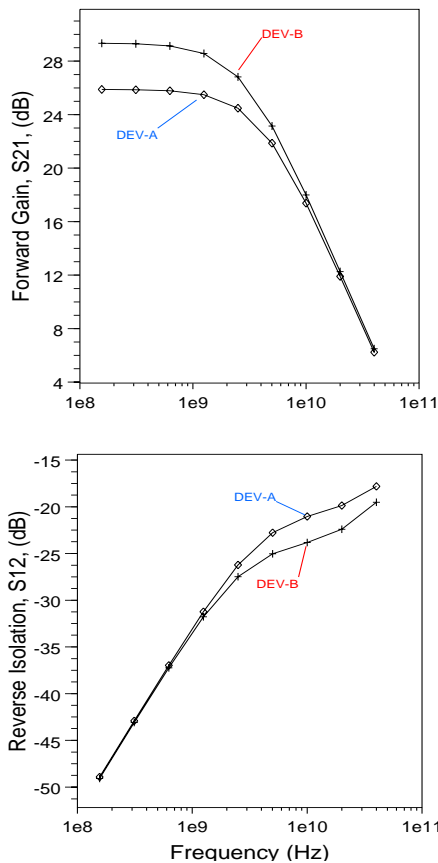


Figure 7: Forward gain, S_{21} (dB), and reverse isolation, S_{12} (dB), for devices DEV-A (rhombus marks) and DEV-B (plus marks) as a function of the frequency.

ACKNOWLEDGMENT

This work is supported by Ministerio de Educación y Ciencia of Spain, grant number TEC2006-11077.

REFERENCES

[1] P. Asbeck, T. Nakamura ed., “Special Issue on Bipolar Transistor Technology: Past and Future Trends”, *IEEE Trans. on Electron Devices*, vol. 48, no. 11, p. 2455, Nov. 2001 .

[2] M. Feng, S-C Shen, D.C. Caruth, J-J Huang, “Device Technologies for RF Front-End Circuits in Next-Generation Wireless Communications”, *Proceedings of the IEEE*, vol. 92, no. 2, pp. 354-375, Feb. 2004.

[3] K. Nellis and Peter J. Zampardi, “A Comparison of Linear Handset Power Amplifiers in Different Bipolar Technologies”, *IEEE Journal on Solid-State Circuits*, vol. 39, no. 10, pp. 1746-1754, Oct. 2004.

[4] T.C.L. Wee, T.C Tsai, J.H. Huang, W.C. Lee, Y.S. Chou, Y.C. Wang, W.J. Ho, “InGaP HBT Technology Optimization for Next Generation High Performance Cellular Handset Power Amplifiers”, *GaAs MANTECH 2005 Gallium Arsenide Manufacturing Technology Conference Proceedings*, 2005.

[5] S-S Myoung, S-H- Cheon, J-G Yook, “Low Noise and High Linearity LNA based on InGaP/GaAs HBT for 5.3 GHz WLAN”, *GAAS2005 Gallium Arsenide Application Symposium Proceedings*, 2005.

[6] J.M. López-González, L. Prat , "The Importance of Bandgap Narrowing Distribution between Conduction and Valence Bands in Abrupt HBTs", *IEEE Trans. on Electron Devices*, vol. 44, no.7 , pp. 1046-1051, July 1997.

[7] J.M. López-González, L. Prat, "Numerical Modelling of Abrupt InP/InGaAs HBTs", *Solid-State Electronics*, vol. 39, no. 4, pp. 523-527, April 1996.

[8] JJ Huang, M. Hattendorf, M. Feng, Q. Hatmann, D. Ahmari, “Material Design and Qualification on Power InGaP HBTs for 2.4 GHz Transmitter Application”, *GaAs MANTECH 2001 Gallium Arsenide Manufacturing Technology Conference Proceedings*, 2001.

[9] C-E Huang,, C-P Lee, H-C Liang, R-T Huang, “Critical Spacing Between Emitter and Base in InGaP Heterojunction Bipolar Transistors (HBTs)”, *IEEE Electron Device Letters*, vol. 23, no. 10, pp. 576-579, Oct. 2002.

[10] www.silvaco.com/products/device_simulation/atlas.html.

[11] J-W. Park, D. Pavlidis, S. Mohammadi, J.L. Guyaux, J-C. Garcia, “Material and Processing Technology for Manufacturing of High Speed, High Reliability InGaP/GaAs HBT based IC’s”, *GaAs MANTECH 1999 Gallium Arsenide Manufacturing Technology Conferenc*, 1999.

[12] Juan M. Lopez-Gonzalez, Antonio J. Garcia-Loureiro, "Physics based model for Tunnel Heterostructure Bipolar Transistors", *Semiconductor Science and Technology*, vol. 19, pp. 1300-1305, 2004.